

See discussions, stats, and author profiles for this publication at: <https://www.researchgate.net/publication/15651094>

Willard DH, Bodnar W & Harris C et al. Agouti structure and function: Characterization of a potent alpha-melanocyte stimulating hormone receptor antagonist. *Biochemistry* 34: 12341-1...

ARTICLE *in* BIOCHEMISTRY · OCTOBER 1995

Impact Factor: 3.02 · DOI: 10.1021/bi00038a030 · Source: PubMed

CITATIONS

80

READS

26

10 AUTHORS, INCLUDING:



[Wanda M Bodnar](#)

University of North Carolina at Chapel Hill

30 PUBLICATIONS 828 CITATIONS

SEE PROFILE

Agouti Structure and Function: Characterization of a Potent α -Melanocyte Stimulating Hormone Receptor Antagonist

Derril H. Willard,[‡] Wanda Bodnar,[§] Cole Harris,[‡] Laura Kiefer,[‡] James S. Nichols,[‡] Steven Blanchard,[‡] Christine Hoffman,[‡] Mary Moyer,[§] William Burkhardt,[§] James Weiel,^{||} Michael A. Luther,[‡] William O. Wilkison,[‡] and Warren J. Rocque*,[‡]

Department of Biochemistry, Department of Bioanalytical and Structural Chemistry, and Department of Cell and Physiology, Glaxo Wellcome, Inc., Five Moore Drive, Research Triangle Park, North Carolina 27709

Received May 18, 1995; Revised Manuscript Received July 6, 1995[®]

ABSTRACT: The murine agouti gene encodes for a novel 131 amino acid protein. The sequence includes a 22 residue putative secretion signal, an internal basic region, and a C-terminal domain containing 10 cysteines. Agouti has been found to antagonize the binding of certain pro-opiomelanocortin peptides, such as α -melanocyte stimulating hormone (α -MSH), to the murine melanocortin-1 receptor (MC1-R). We report the purification of a secreted murine agouti to homogeneity by a two-step procedure from baculovirus-infected *Trichoplusia ni* (*T. ni*). The protein is glycosylated and exhibits competitive, high-affinity antagonism ($K_i = 0.8$ nM) versus α -MSH in cell-based assays employing B16F10 cells. Association state analysis by analytical ultracentrifugation reveals that agouti exists in a monomer–dimer plus aggregate equilibrium at low micromolar concentrations. Data from secondary structure studies indicate that the protein is highly stable to thermal denaturation. Enzymatic digestion to probe disulfide bond arrangement yielded a discrete C-terminal (Val 83–Cys 131) domain. The isolated highly cysteine-rich C-terminal domain retains α -MSH antagonism equipotent with mature agouti. This bioactive domain contains all 10 cysteines which exhibit sequence homology when aligned with several conotoxins.

The murine agouti gene encodes for a novel 131 amino acid (aa)¹ agouti protein. The sequence contains a 22 aa putative secretion signal, a putative N-linked glycosylation motif flanking Asn 39, and a lysine-rich basic region. The carboxyl-terminal portion of the sequence contains 10 cysteines with the potential to form 5 disulfide bonds. Recently, the human homolog of the agouti gene containing a high degree of identity was discovered (Kwon et al., 1994). Scans of protein sequence databases have indicated that agouti is a novel protein with no strong identity or homology to other known families.

The agouti gene is normally expressed in the skin of wild-type mice between the third and seventh day after birth. However, mice bearing the lethal yellow mutation (A^y) express mRNA in many tissues, including testis, liver, spleen, and skin (Michaud et al., 1993, 1994). The homozygous condition is lethal prior to zygote implantation. Heterozygotes exhibit a host of pleiotropic effects, the most obvious of which is the yellow coat color resulting from agouti-induced production of pheomelanin and inhibition of eumelanin [Bultman et al., 1992; Robbins et al., 1993; reviewed in Yen et al. (1994)]. Other observed effects

include the characteristic insulin-resistant diabetes, a tendency to develop tumors, and the pathological obesity found in these mice.

Agouti has been found to antagonize the binding of α -MSH and certain other pro-opiomelanocortin peptides to MC1-R and the murine melanocortin-4 receptor (Lu et al., 1994). The specificity of interaction between the melanocortin receptors and their peptide ligands depends on slight variations of the ligands' highly conserved amino acid sequences. Although agouti does not contain a region of high identity or homology with this group of peptides, the high-affinity antagonism indicates the presence of a potent binding epitope. The specific residues involved in agouti binding to the receptor are unknown.

The occurrence of agouti in conjunction with diabetes, tumor frequency, and obesity in mice provides a model for the further study of these disease states. The ability to monitor agouti antagonism of melanocortin receptors furnishes a simple mechanism for probing agouti function. Additionally, the publication of the human gene and the identification of human agouti mRNA in testis and adipose tissue provide a possible correlation with the same diseases in man. Native sources of agouti yielding sufficient amounts of protein for extensive experimentation have yet to be identified. We utilized a large-scale baculovirus system to produce milligram quantities of recombinant agouti and purified the protein to homogeneity. Mass spectral and N-terminal sequence analyses revealed processing of the signal sequence, identification of multiple N-linked glycoforms, and the presence of five disulfide bonds. Analysis by circular dichroism indicated that the protein exhibited reversible heat denaturation. Enzymatic digestion yielded a discrete C-terminal domain that retained equivalent α -MSH

* To whom correspondence should be addressed. Telephone: (919) 941-3106. Fax: (919) 941-3411. E-Mail: WJR6556@USAV01.GLAXO.COM.

[‡] Department of Biochemistry.

[§] Department of Bioanalytical and Structural Chemistry.

^{||} Department of Cell and Physiology.

[®] Abstract published in *Advance ACS Abstracts*, September 1, 1995.

¹ Abbreviations: aa, amino acid(s); A^y , lethal yellow mutation; MC1-R, melanocortin-1, receptor; α -MSH, α -melanocyte stimulating hormone; Sf-9, *Spodoptera frugiperda* cells; *T. ni*, *Trichoplusia ni*; MOI, multiplicity of infection; PVDF, poly(vinylidene difluoride); PTH, phenylthiohydantoin.

antagonism to that exhibited by intact agouti in cell-based assays.

EXPERIMENTAL PROCEDURES

Expression and Fermentation Conditions of Agouti. Briefly, murine agouti cDNA yielded a 614 bp *XbaI/PstI* fragment. The fragment was subcloned into the baculovirus vector pAcMP3 (PharMingen, San Diego, CA), under control of the basic promoter. Viruses incorporating this vector were produced by standard methods (Summers & Smith, 1987; O'Reilly et al., 1992).

Spodoptera frugiperda cells (Sf-9) obtained from ATCC (Rockville, MD) were propagated as suspension cultures in Grace's supplemented medium containing 10% fetal bovine serum and 0.1% pluronic F-68 and were used to produce a large-scale high-titer virus stock. Cells were infected at a density of 1×10^6 /mL with a MOI of 0.1 plaque forming unit/cell. Virus was harvested 72 h post-infection, and the titer was determined by plaque assay as previously described (Summer & Smith, 1987). Fifteen liter scale production runs of murine agouti were produced using *Trichoplusia ni* (*T. ni*) High Five cells, adapted to suspension (kindly obtained from JRH Biosciences, Woodland, CA). *T. ni* cells, grown in Excel 405 medium containing 50 μ g/mL gentamicin, were inoculated into a 15 L stirred vessel. Cells were infected 24 h post-seeding at a density of 1×10^6 cells/mL with a MOI of 1 plaque forming unit/cell. Cells were harvested 48 h post-infection and retained 92% viability.

Purification. Media from a 15 L fermenter were prepared by filtration through a Whatman 3 filter. Agouti was followed during the purification by the presence of an overexpressed band at ~18.5 kDa on SDS-PAGE and visualized by ISS ProBlue (Integrated Separation Systems, Natick, MA) staining and by antagonism of adenylate cyclase stimulation as described below. Working protein concentrations were determined throughout the experiments using the BCA Protein Assay kit (Pierce, Rockford, IL).

A 20 mL Poros 20 HS cation-exchange column (26 mm \times 40 mm) was equilibrated with 50 mM NaCl, 20 mM PIPES, pH 6.5. The medium was loaded directly onto the column at 10 mL/min using a Pharmacia BioPilot system and then washed to base line with equilibration buffer. Bound proteins were step-eluted with increasing NaCl concentrations to 1 M NaCl in the equilibration buffer. Agouti protein was present in the 0.8 M NaCl fraction. The agouti-containing fraction was concentrated using a Filtron 5 kDa molecular weight cutoff 10 mL disposable membrane stirred cell. The concentrate was diluted 1:1 with 0.1% TFA/H₂O (buffer A), and 0.1% TFA/acetonitrile (buffer B) was added to 5%. Samples were loaded onto a Poros II R—column (10 mm \times 100 mm, stainless steel) in 95% buffer A, 5% buffer B, and chromatographed to 20% buffer A, 80% buffer B. Peaks were monitored at 220 nm. Agouti eluted at 22% buffer B. The fractions containing agouti were pooled, shell-frozen, and lyophilized. Protein was resuspended post-lyophilization in PBS or 150 mM NaCl, 20 mM borate, pH 8.0.

N-Terminal Sequencing. For initial identification of agouti, analyses were performed by electrophoresing samples on a Novex 4–20% Tris/glycine mini-gel (100 mm \times 100 mm \times 1 mm). Proteins were then electroblotted onto Trans-Blot PVDF (Reim & Speicher, 1993) using a Hoefer TE 22

Mini-Transphor unit. Following transfer, proteins were stained with 0.1% amido black in 50% methanol. Agouti proteins were excised, inserted into a Hewlett-Packard (HP) membrane-compatible cartridge, and subjected to N-terminal Edman sequencing using the HP G1000A Protein Sequencer with HP 1090 HPLC for on-line PTH analysis. Subsequently, purified agouti samples were taken directly to an HP reverse phase support. Sequencing was performed as above.

N-Terminal sequencing was also used to analyze disulfide pairing via a modification of an *in situ* S-pyridylethylation technique (Morita et al., 1992; Zhang & Liang, 1993). First and second half-cystines of intact cystinyl pairs were designated by the detection or absence of PTH derivatives at known cysteine positions.

Amino Acid Composition Analysis. Amino acid composition was determined from triplicate samples of agouti dialyzed into 150 mM NaCl, 20 mM borate buffer, pH 8.0. Gas phase hydrolysis with 6 N HCl was carried out for 1 h at 150 °C. Amino acid yields were determined using an Applied Biosystems 420A Derivatizer with a 130A Separation System and a 920A Data Analysis Module.

Mass Spectral Analysis. Samples (50–200 pmol) were analyzed by liquid chromatography electrospray ionization mass spectrometry on a Sciex API III triple quadrupole instrument (Thornhill, Ontario). Predicted masses were calculated from primary sequence analysis using the Compost software package. Peptides were eluted directly into the mass spectrometer from microcapillary columns (300 μ m and 800 μ m \times 100 mm; LC Packings, San Francisco, CA) using an acetonitrile/TFA (buffer A, 0.05% TFA/H₂O; buffer B, 90% acetonitrile/0.045% TFA) linear gradient from 0 to 60% buffer B in 10 min. The mass range 500–1500 atomic mass units was scanned every 3 s with a needle voltage of 5000 V and an orifice potential of 70 V.

For glycoform analysis, determination of the oxidative state of cysteine residues, and identification of the binding region, intact murine agouti was digested with sequencing grade endoproteinase Lys-C or Asp-N (Boehringer Mannheim, Indianapolis, IN) in PBS with a 1:20 enzyme to agouti ratio (w/w). Incubations were carried out overnight at 37 °C. Peptides were isolated by HPLC for mass analysis.

Adenylate Cyclase Assay. B16F10 cells obtained from Dr. David Emerson (Department of Pharmacology, Glaxo Wellcome, Inc.) were cultured in RPMI 1640 supplemented with 2 mM glutamine, 50 units/mL penicillin, 50 μ g/mL streptomycin, and 10% fetal bovine serum in a humidified 5% CO₂, 95% air atmosphere. The cells were plated into 96-well round-bottom tissue culture plates at a density of either 1×10^5 or 2.5×10^4 cells/well 1 or 2 days before use, respectively. The final cell density on the day of the experiment was approximately 10^5 cells/well. For assessment of the ability of agouti to inhibit cAMP accumulation induced by α -MSH (1 nM), cell monolayers were washed with RPMI-1640 containing 1 mg/mL bovine serum albumin. Both the α -MSH and the agouti samples were diluted in the previous buffer with 0.6 mM 3-isobutyl-1-methylxanthine added. Cells were incubated with the varying concentrations of agouti in a final volume of 200 μ L/well at 37 °C. The reaction was allowed to proceed for 1 h followed by addition of 50 μ L/well of 50 mM sodium acetate (pH 4) containing 0.1% Triton X-100. The plates were then heated at 90 °C for 5 min to stop cellular cAMP production. Samples were

either assayed immediately or stored frozen. The cAMP content of the samples was determined by scintillation proximity assay using a commercially available kit (Amersham, Arlington Heights, IL). K_i 's were determined by fitting the data to a competitive inhibition model using a nonlinear least-squares analysis.

Binding Assay. B16F10 monolayers cultured as described above were washed with RPMI 1640 containing 50 mM HEPES, pH 7.5, and 1 mg/mL BSA. Cells were incubated with [125 I]-NDP- α -MSH (0.067 nM) and wild-type (0.3–259 nM) or C-terminal (0.3–300 nM) agouti in the same media with gentle agitation for 2 h at room temperature (total volume = 100 μ L). Samples were cooled on ice, and the medium containing free ligand and antagonist was removed by rapid aspiration. Cells were washed twice with 125 μ L of ice-cold PBS, and 125 μ L of scintillation cocktail was added. Bound radioactive ligand was measured using a Wallac 1650 Microbeta plate counter.

Data were fit to eq 1 where cpm_{tot} is the value in the absence of antagonist and I is wild-type or C-terminal agouti. Additionally, the value for nonspecific binding was determined by addition of 1 μ M agouti and was subtracted from all data.

$$\text{cpm}/\text{cpm}_{\text{tot}} = \text{cpm}_{\text{max}}[1 - ([I]/(IC_{50} + [I]))] \quad (1)$$

IC_{50} values were converted to inhibition constants (K_i) using the Cheng–Prusoff equation (eq 2) where L is [125 I]-NDP- α -MSH and $K_D = 0.02$ nM for NDP- α -MSH/receptor binding.

$$K_i = IC_{50}/(1 + [L]/K_D) \quad (2)$$

Analytical Ultracentrifugation. Sedimentation equilibrium analytical ultracentrifugation on secreted agouti and the isolated C-terminal domain (Val 83–Cys 131) was performed using a Beckman XL-A (Palo Alto, CA) centrifuge with two-channel 12 mm charcoal-filled epon centerpieces. Runs were performed on secreted agouti at 15 000, 17 500, 20 000, 22 500, and 25 000 rpm at 4 and 20 $^{\circ}$ C with scans taken at 220 nm at 1 h intervals. Data on the C-terminal domain were taken at 20 000, 25 000, and 30 000 rpm at 4 $^{\circ}$ C. Equilibrium was judged to be achieved by the absence of change between plots of several successive scans after approximately 20 h; 180–200 μ L of each sample in 300 mM NaCl, 20 mM borate, pH 8.0, was centrifuged against 250 μ L of the equivalent buffer blank. Initial protein concentrations were 0.023–0.34 mg/mL. Solvent density was determined empirically at 4 and 20 $^{\circ}$ C using a Mettler DA-110 density/specific gravity meter calibrated against water. The partial specific volume of each protein was calculated using the method of Cohn and Edsall (1943). Temperature differentials were incorporated using the appropriate equation (Laue et al., 1992) modified from values of each amino acid at 25 $^{\circ}$ C (Durschlag, 1986). The partial specific volume was further modified according to the weight percentage of glycosylation using the best estimate of sugar identity from mass spectral analysis. Data sets were obtained as radial distance versus absorbance and later converted to concentration units using an empirically derived extinction coefficient. Raw data were analyzed by the Beckman/Microcal Origin nonlinear regression software package using multiple iterations of the Marquardt–Levenberg algorithm

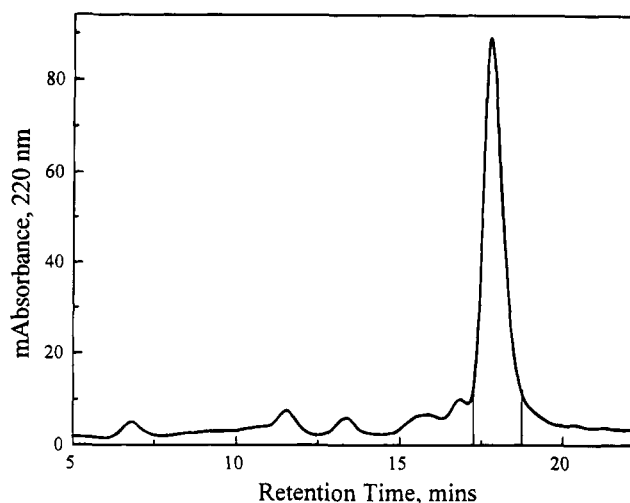


FIGURE 1: HPLC chromatogram of agouti purification. Cation exchange fractions containing agouti were chromatographed on a Poros II R/M column. The delineated peak denotes agouti elution at 22% acetonitrile. Absorbance was monitored at 220 nm.

(Marquardt, 1963) for parameter estimation or by global fitting routines kindly provided by the National Analytical Ultracentrifuge Facility at Storrs, CT.

Secondary Structural Determination Using Circular Dichroism. Purified mouse agouti protein at 0.3 mg/mL in 150 mM NaCl, 20 mM borate buffer, pH 8.0, was examined by CD spectroscopy on an Aviv Model 62DS CD spectropolarimeter (AVIV Associates, Lakewood, NJ). The protein was repetitively scanned in 0.1 cm quartz cuvettes at 20 and 80 $^{\circ}$ C from 250 to 198 nm in 0.2 nm increments. A 1.5 nm bandwidth and 0.5 s averaging time were used. A total of five scans were averaged and corrected for buffer contributions. The data were fit to a single Lorentzian distribution for representation. Thermal melts of the protein were performed from 20 to 80 $^{\circ}$ C in 1 $^{\circ}$ C increments while monitoring at 205 nm.

RESULTS

Purification and Characterization of Agouti Protein. We utilized a *T. ni* baculovirus system which efficiently secreted active protein into the surrounding media. Cells exhibited 92% viability at the time of harvest, indicating that agouti production had no apparent toxic effects. Protein expression levels were extrapolated post-cation-exchange chromatography to 0.5 mg/L media.

On the basis of the calculated pI of the agouti sequence (pI 9.8), a cation-exchange column was run at pH 6.5. The 0.8 M NaCl eluant fraction yielded an 18.5 kDa protein enriched to 80–90% purity by SDS–PAGE that reacted positively on Western blot analysis using rabbit polyclonal antibodies produced to residues 25–40 (data not shown). Further purification was obtained by reverse-phase HPLC (Figure 1). Substantial losses were observed during this step (>50% at times). Purity levels were increased to >99% as determined by SDS–PAGE, N-terminal Edman sequencing, and mass spectral analysis. Post-HPLC and lyophilization, purified agouti exhibited competitive antagonism versus α -MSH in our adenylate cyclase assay. In either PBS or borate buffer, the K_i was determined to be 0.8 nM. Agouti was found to have an IC_{50} of 15.4 ± 2.0 nM in our binding assay. Conversion of the IC_{50} to a K_i using the Cheng–Prusoff equation produced a value of 4.6 ± 0.6 nM.

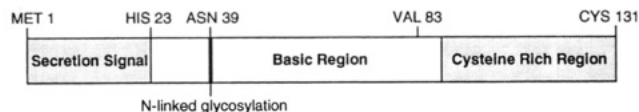


FIGURE 2: Depiction of the primary structure of murine agouti. The agouti sequence includes a secretion signal, a predominantly basic region loosely defined from His 23 to Lys 82 containing an N-linked glycosylation site, and a C-terminal cysteine-rich region.

N-Terminal Edman sequencing indicated that our secreted construct began at His 23, confirming that the 22 residues N-terminal to His 23 had been processed (Figure 2). Sequencing also failed to identify an amino acid at the expected position of Asn 39, suggesting that post-translational modification had occurred at the predicted N-linked glycosylation site, consistent with the purified agouti having a larger apparent mass than predicted (assuming five disulfide bonds and no other modifications, 11 837 Da).

To determine the nature and location of the various contributions to the protein's molecular weight, enzymatic digestion and peptide isolation were performed. Analysis of peptides generated by Asp-N cleavage indicated that the mass differences were solely due to peptides which contained Asn 39. Subsequent mass spectral analysis of the intact protein yielded a heterogeneous mix of ions corresponding to species with molecular masses of 12 860, 13 022, and 13 225 Da. The differences between the three masses correspond to the addition of hexosamine and hexose sugars, respectively, agreeing with our interpretation of the aberrant mobility on SDS-PAGE and N-terminal Edman sequencing results. Attempts to remove sugar moieties using glycopeptidase F to resolve the protein to its predicted molecular weight were unsuccessful.

Association State. Sedimentation equilibrium experiments were performed to determine the association state of agouti. Samples were prepared in a NaCl/borate buffer to allow direct amino acid composition analysis not possible with samples in phosphate buffer. A best-fit model corresponding to a monomer-dimer plus aggregate equilibrium was produced from data collected at two temperatures, two concentrations, and multiple speeds for the intact agouti. At experimental concentrations, $\geq 30\%$ of the agouti existed as large, indeterminate aggregates and was depleted from the cell over the experimental velocity range (15 000–25 000 rpm). From the absorbance-dependent association constant and the experimentally derived molar extinction coefficient (184 773 at 220 nm), a K_D of $3.0 \mu\text{M}$ was calculated for the monomer-dimer equilibrium. Using a direct $N \rightleftharpoons N_2$ equilibrium model and the calculated K_D , a weight-average species distribution plot was produced to facilitate predictions on percent monomer over a concentration range (Figure 3).

Analysis of Secondary Structure and Stability. We performed circular dichroism studies in order to examine the secondary structure and thermal stability of agouti. Replicate average spectra obtained at 20°C indicated a minimum molar ellipticity at 201 nm (Figure 4). The far-UV CD spectra indicated a small percentage of α -helix and β -sheet structure with a large contribution of irregular, less-defined structure. These results contradict secondary structure predictions where a larger α -helical content is expected. Heating agouti to 80°C produced a slight blue shift in the CD spectrum. When the same sample was cooled to 20°C and rescanned, the spectrum was identical to the original 20°C scan. The

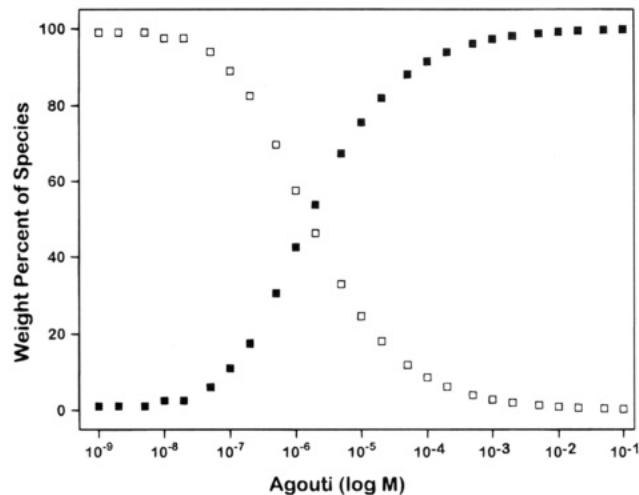


FIGURE 3: Weight fraction distribution of monomer-dimer species vs log of molar agouti concentration. (\square) denotes percent monomer. (\blacksquare) denotes percent dimer. Curves were generated from 4°C data at 5 speeds. $K_D = 3.0 \mu\text{M}$.

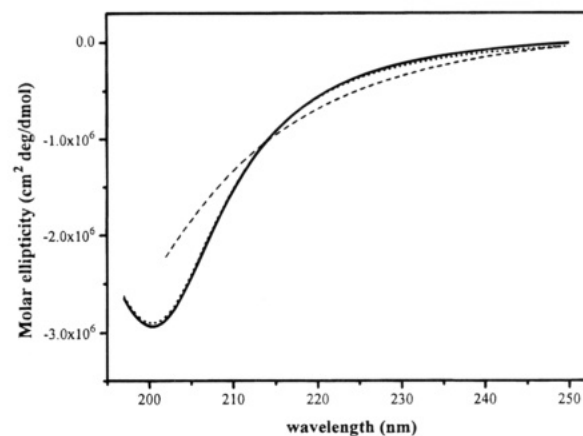


FIGURE 4: Circular dichroism scans of native (—), heat-denatured (---), and renatured (···) agouti. Five replicate scans of agouti from 197 to 250 nm were averaged. The resulting data were converted into molar ellipticity and fit to a Lorentzian distribution for representation. Native and renatured agouti were scanned at ambient temperature. Denatured protein was incubated at 80°C for 1 h and scanned.

protein from this experiment was assayed for its ability to antagonize α -MSH-induced cAMP elevation and was found to retain initial activity levels.

Examination of Disulfide Bonds. We probed the oxidation state of the 10 cysteines using several techniques. Initial results using a micro-Ellman's assay indicated that agouti did not contain any free sulfhydryls. Lys-C digests yielded a C-terminal fragment, Val 83–Cys 131, that was isolated by HPLC. The mass of this peptide (5088 Da) was consistent with the predicted mass assuming all 10 cysteines were involved in disulfide bonds. A modified *in situ* S-pyridylethylation N-terminal sequencing technique was employed to probe disulfide pair arrangement using the isolated C-terminal domain. Data generated by the absence or the detection of PTH-modified cystinyl half-residues allowed us to designate each cysteine as a "one" (sequentially N-terminal) or "two" (C-terminal).

Characterization of the C-Terminal Domain. The ability of the C-terminal domain to antagonize the α -MSH receptor was tested in both the adenylate cyclase and the direct binding assays. As shown in Figure 5, the truncate was

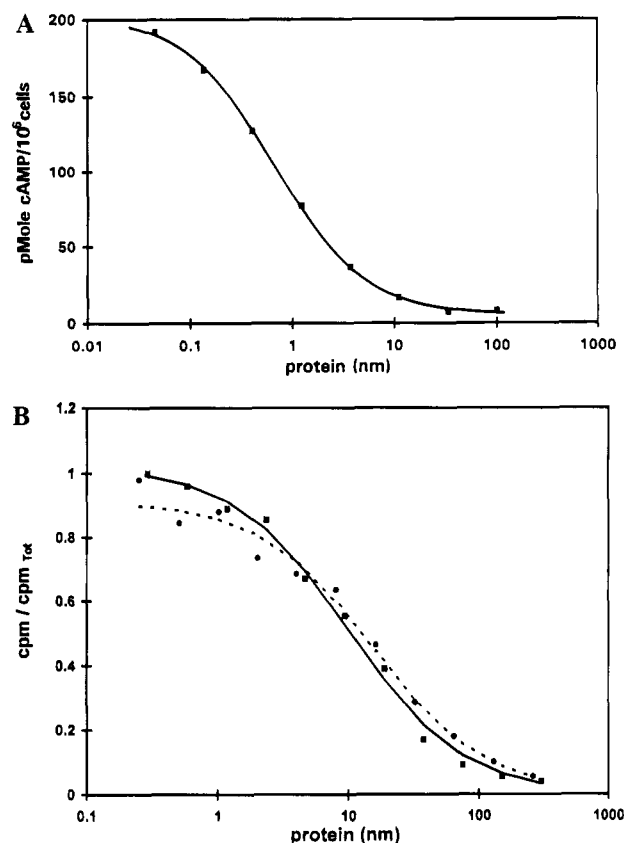


FIGURE 5: Potency of receptor antagonism and binding of the agouti C-terminal domain: (A) cAMP levels were determined in B16F10 cells induced by constant (1 nM) α -MSH and treated with serial dilutions of the isolated C-terminal domain. K_i was determined by plotting protein concentration vs picomoles of cAMP and fitting the data to a competitive inhibition model by a nonlinear least-squares method. (B) Inhibition of [¹²⁵I]-NDP- α -MSH binding to B16F10 cells was determined by incubating cells with increasing concentrations of wild-type (●, 0.3–259 nM) or C-terminal (■, 0.3–300 nM) agouti in the presence of 0.067 nM [¹²⁵I]-NDP- α -MSH. The data were fit to eq 1, yielding IC₅₀ values of 15.4 ± 2.0 nM for wild type (---) and 10.0 ± 0.8 nM for C-terminal (—) agouti which were converted to K_i values of 4.6 ± 0.06 nM (wild type) and 3.0 ± 0.2 nM (C-terminal).

found to exhibit antagonism in both systems. The calculated K_i for the C-terminal domain was determined to be 0.79 nM in the adenylate cyclase assay, equivalent to that derived for mature agouti. The K_i for antagonism of [¹²⁵I]-NDP- α -MSH binding was 3.0 ± 0.2 nM, similar to that observed for full-length agouti. Sedimentation equilibrium studies performed on the isolated C-terminus revealed that the domain exists as a monomer at the experimental concentration.

DISCUSSION

The association of agouti with multiple pathologies makes an in-depth understanding of the protein's structure and function therapeutically relevant. For the purpose of our studies, a recombinant system was needed that would support the production of milligram quantities of protein. We found that the *T. ni* system expressed sufficient levels of agouti in a secreted, active form. Our two-column purification yielded protein of >99% purity which displayed low nanomolar α -MSH antagonism. Initially, substantial losses of protein occurred during chromatographic and concentration steps. We attribute this to the hydrophobic characteristics of the protein, although a cursory scan of the primary sequence

did not indicate that the protein would be unusually hydrophobic. The addition of 0.1% Triton X-100 (inappropriate for most of our studies) was found to increase protein recovery. N-Terminal Edman sequencing of partially purified fractions confirmed that the 22 residue secretion signal had been cleaved from the protein. Subsequent mass spectral analyses revealed that Asn 39 was an N-linked glycosylation site and accounted for the discrepancy between SDS-PAGE analysis and predicted molecular weight.

Sedimentation experiments indicated that agouti exists in solution as a monomer-dimer equilibrium at low micromolar concentrations. The derived K_D for the monomer-dimer association predicts that agouti would exist primarily as a monomer at the nanomolar ranges used in both the adenylate cyclase and binding assays. Since agouti is active as an α -MSH receptor antagonist at the nanomolar level, we would argue that the monomer species is sufficient for activity. The finding that the C-terminal domain exists as an ideal monomer and also retains full antagonism supports a model for agouti functioning as a monomer. However, we cannot rule out multimerization effects induced by *in vivo* conditions, such as locally high concentrations, cofactors, or receptor binding.

Secondary structure analysis by the Chou and Fasman (1978) method predicted the presence of two α -helical regions; one involving His 23–Leu 30 (the N-terminus of the secreted protein) and the second spanning most of the lysine-rich region (Figure 2). Additionally, the residues flanking Asn 43 strongly resemble a helical N-cap (Harper & Rose, 1993) and precede the second predicted helical region. However, the CD spectrum of the intact protein reveals very little α -helical content. During labeling attempts using the Bolton-Hunter method, we were largely unable to modify lysine residues in this region. This resistance to labeling may indicate that these residues are buried or alternatively masked by glycosylation.

A discrete C-terminal domain was produced while we were probing the oxidation state of the 10 cysteines. This truncate provided an avenue for preliminary structure/function analysis. We were able to localize the α -MSH antagonist epitope to the C-terminal domain as judged by the equipotent antagonism of the intact wild-type and truncated protein in both the adenylate cyclase and binding assays. These findings indicate that the C-terminal region is directly involved in receptor binding. The role of the N-terminal portion is not known but is a subject of current investigation.

Disulfide bonds are a common feature of many extracellular proteins and presumably serve to stabilize the native conformation by lowering the entropy of the unfolded form (Anfinsen & Scheraga, 1975). The thermal stability of wild-type agouti activity most probably results from the rigidity imparted to the C-terminal domain by the five disulfide bonds. Since agouti is believed to normally produce a paracrine effect, such innate structural stability is not surprising.

As shown in Figure 6, the C-terminal region of agouti exhibits cysteine spacing in common with the conotoxin family of neural toxins (Hillyard et al., 1989; Shon et al., 1994). All six cysteines in the conotoxins are known to exist as disulfide pairs. Data obtained from the absence or detection of the PTH-cysteine derivative during N-terminal sequencing of agouti allowed us to designate each half-cysteine as a "one" (sequentially N-terminal) or "two" (C-

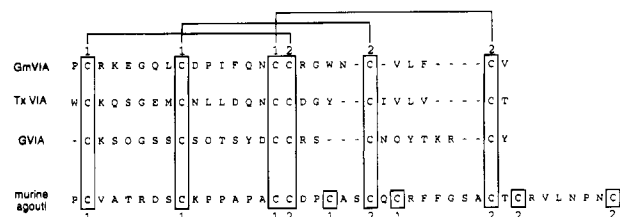


FIGURE 6: Primary sequence alignment of agouti and several conotoxins. Boxes indicate positions of cysteine alignment. The order of sequences is as follows: aa 3–29 of the conotoxin Gm VIA (*Conus glorimaris*); aa 1–27 of the conotoxin Tx VIA (*C. textile*); aa 1–27 of the conotoxin GVIA (*C. geographus*); and aa 91–131 murine agouti. Brackets denote disulfide arrangement of the conotoxins. Numerals indicate identification of individual cysteines as the N-terminal (1) or C-terminal (2) partner of a disulfide pair.

terminal). When the conotoxin disulfide arrangement is compared with our assessment of agouti half-cystines, the spacing and sequential designation of the first four cysteines match exactly. We compared subsequent cysteines solely by sequential designation. Our suggested alignment requires the introduction of gaps into the conotoxin sequences and reflects one possible interpretation.

Interestingly, agouti and the conotoxins exhibit effects on cellular calcium levels. The conotoxins are potent calcium channel antagonists and derive their toxicity by blocking calcium flux into cells. Agouti has the ability to elevate intracellular calcium levels in a variety of cell types (Zemel et al., 1995). While these actions are apparently opposing, it is intriguing that proteins which share a structural motif also function as extracellular agents affecting calcium regulation. We are presently studying the effect of agouti in relation to several disease models.

ACKNOWLEDGMENT

After this paper was submitted for publication, a commentary was published by Manne et al. (1995) which also included a homology comparison of agouti and conotoxins.

REFERENCES

- Anfinsen, C. B., & Scheraga, H. A. (1975) *Adv. Protein Chem.* 29, 205–299.
- Bultman, S. J., Michaud, E. J., & Woychik, R. P. (1992) *Cell* 71, 1195–1204.
- Chou, P. Y., & Fasman, G. D. (1978) *Annu. Rev. Biochem.* 47, 251–276.
- Cohn, E. J., & Edsall, J. T. (1943) in *Proteins, amino acids and peptides as ions and dipolar ions*, p 157, Reinhold, New York.
- Durschlag, H. (1986) in *Thermodynamic data for biochemistry and biotechnology* (Hinz, H. J., Ed.) p 45, Springer-Verlag, New York.
- Harper, E. T., & Rose, G. D. (1993) *Biochemistry* 32, 7605–7609.
- Hillyard, D. R., Olivera, B. M., Woodward, S., Corpuz, G. P., Gray, W. R., Ramilo, C. A., & Cruz, L. J. (1989) *Biochemistry* 28, 358–361.
- Kwon, H. Y., Bultman, S. J., Loffler, C., Chen, W.-J., Furdon, P. J., Powell, J. G., Usala, A.-L., Wilkison, W., Hansmann, I., & Woychik, R. P. (1994) *Proc. Natl. Acad. Sci. U.S.A.* 91, 9760–9764.
- Laue, T. M., Shah, B. D., Ridgeway, T. M., & Pelletier, S. L. (1992) in *Analytical ultracentrifugation in biochemistry and polymer science* (Harding, S. E., Rowe, A. J., & Horton, J. C., Eds.) p 102, The Royal Society of Chemistry, Cambridge, U.K.
- Lu, D., Willard, D., Patel, I. P., Kadwell, S., Overton, L., Kost, T., Luther, M., Chen, W., Woychik, R. P., Wilkison, W. O., & Cone, R. D. (1994) *Nature* 371, 799–802.
- Manne, J., Argeson, A. C., & Siracusa, L. (1995) *Proc. Natl. Acad. Sci. U.S.A.* 92, 4721–4724.
- Marquardt, D. W. (1963) *J. Soc. Ind. Appl. Math.* 11, 431–441.
- Michaud, E. J., Bultman, S. J., Stubbs, L. J., & Woychik, R. P. (1993) *Genes Dev.* 7, 1203–1213.
- Michaud, E. J., Bultman, S. J., Klebig, M. L., van Vugt, M. J., Stubbs, L. J., Russell, L. B., & Woychik, R. P. (1994) *Proc. Natl. Acad. Sci. U.S.A.* 91, 2562–2566.
- Morita, N., Yamaguchi, M., & Nohkura, K. (1992) *J. Protein Chem.* 11, 362.
- O'Reilly, D. R., Miller, L. K., & Luckow, V. A. (1992) in *Baculovirus expression vectors. A laboratory manual*, W. H. Freeman, New York.
- Reim, D., & Speicher, D. (1993) *Anal. Biochem.* 214, 87–95.
- Robbins, L. S., Nadeau, J. H., Johnson, K. R., Kelly, M. A., Rosselli-Rehfs, L., Baack, E., Mountjoy, K. G., & Cone, R. D. (1993) *Cell* 72, 827–834.
- Shon, K.-J., Hasson, A., Spira, M. E., Cruz, L. J., Gray, W. R., & Olivera, B. M. (1994) *Biochemistry* 33, 11420–11425.
- Summers, M. D., & Smith, G. E. (1987) *Tex., Agric. Exp. Stn., Bull.* 1555, 29–31.
- Yen, T. T., Gill, A. M., Frigeri, L. G., Barsh, G. S., & Wolff, G. L. (1994) *FASEB J.* 8, 479–488.
- Zemel, M., Kim, J., Woychick, R., Michaud, E., Kadwell, S., Patel, I., & Wilkison, W. (1995) *Proc. Natl. Acad. Sci. U.S.A.* 92, 4733–4737.
- Zhang, D., & Liang, S. (1993) *J. Protein Chem.* 12, 735–740.

BI951123C